# Complexity measure by ordinal matrix growth modeling

J. S. Armand Eyebe Fouda[a,b], Wolfram Koepf[b]

[a]*Department of Physics, Faculty of Science, University of Yaoundé I, P.O. Box 812, Yaoundé, Cameroon*
[b]*Institute of Mathematics, University of Kassel, Heinrich-Plett Str. 40, 34132 Kassel, Germany*

## Abstract

We present a new approach based on the modeling of the behavior of the number of ordinal matrices derived from time series, as a function of the embedding dimension. We show that the number of distinct ordinal matrices can be used for determining whether the dynamics are regular or chaotic by means of the periodicity ($\mu$), quasi-periodicity ($\alpha$) and nonregularity ($\lambda$) index herein defined. We verify that $\lambda$ behaves similarly to the Lyapunov exponent and therefore can be used for measuring complexity in time series whose underlying equations are unknown. Moreover, the combination of $\mu$, $\alpha$ and $\lambda$ enables us to distinguish between deterministic and stochastic data. We thus propose the variation law of the number of ordinal matrices characterizing the random walk.

*Keywords:* complexity, ordinal matrix, Lyapunov exponent

## 1. Introduction

Measuring complexity from time series is crucial for understanding the internal behavior of dynamical systems, and is applied in diverse fields of research such as physics, finance and economics, biology, and meteorology [1–4]. Among the existing methods, ordinal pattern-based algorithms (OPA) have been shown effective as they can be easily applied to any type of data series, and are computationally low cost. Bandt and Pompe showed in their basic paper [5] that the permutation entropy (PE) behaves similarly to the Lyapunov exponent (LE) for chaotic dynamics. However, in the case of regular dynamics, the PE outputs positive values, whereas the corresponding Lyapunov exponent is negative. Indeed, in information theory, periodic dynamics contain no information and their entropy therefore should be zero. The PE thus fails to characterize regular dynamics.

In order to address this concern, improvements of the PE have been undertaken [6–13]. One can particularly quote the conditional entropy of ordinal patterns (CPE) and the permutation largest slope entropy (PLSE) [14, 15]. The first algorithm is a detection approach while the second one is a complexity measure. The PLSE allows to detect regular dynamics with a zero entropy as

the algorithm can handle large embedding dimensions with moderate computation time, but it cannot be considered as a complexity measure. Unakafov and Keller showed that CPE approximates better the Kolmogorov-Sinai entropy (KSE) [14]. Although the CPE lets us easily detect periodic dynamics with a zero complexity, the required embedding dimension ($n$) increases as the period of the underlying dynamics is large. Given that the required observation time increases as $n!$, only periodic dynamics with small periods can be properly detected with a zero complexity. In their fast CPE algorithm for example, Unakafov and Keller have considered only $n = 8$ as the largest embedding dimension.

Recently, we proposed the ordinal array complexity (OAC) as a generalized approximation of the KSE by considering arrays of permutations as patterns [16]. We showed that the possible number of ordinal arrays (OA) increases as a power of $n!$. Indeed, for ordinal arrays containing $m$ permutations of order $n$, the maximum number of ordinal arrays that can be derived from a time series is $\Lambda_0 = (n!)^m$. The CPE is thus obtained by setting $m = 2$. However, although $\Lambda_0$ is accurately determined, the number of OA that is derived from a given observation is not known a priori and depends on the nature of the time series. We showed for example in [15] that in the case of periodic dynamics with nonrepeating values in the basic period, the number of ordinal patterns does not exceed $L$, where $L$ is the phase space period of the underlying time series. In the case of chaotic dynamics, $\Lambda$ depends on the complexity of the dynamics and for large values of $m$, $\Lambda = \Lambda_0$ is reached only with purely random sources. From these observations, it then turns out that evaluating $\Lambda$ can give additional inputs for the complexity measure.

In this paper, we propose modeling the behavior of $\Lambda$ in terms of $m$. Three ordinal matrix-based chaos indicators (OMCI) are thus derived, namely the periodicity, the quasi-periodicity and the nonregularity index. The nonregularity index particularly behaves similarly to the Lyapunov exponent (LE), thus taking negative values for regular dynamics and positive values for nonregular dynamics. The other indicators help to determine whether a dynamics is periodic or quasi-periodic, or even stochastic. The rest of the paper is organized as follows: in Sect. 2 we present the modeling equation of $\Lambda$; Sect. 3 is devoted to simulation results while some concluding remarks are given in Sect. 4.

## 2. Ordinal matrix-based chaos indicators

### 2.1. Brief recap of the ordinal matrix transform

We introduced in [16, 17] the ordinal array transform in which the time series is transformed into a series of ordinal patterns (permutations), which itself is transformed into a series of ordinal arrays by embedding permutations. In this section, we limit the transform to 2-dimensional arrays (matrices). Let $\{x_t\}_{t=0,1,\ldots,T-1}$ be a time series of length $T$ where $t$ is the time index. Permutations of order $n$ are obtained by sorting into increasing order the values in embedding vectors $\mathbf{x}_k = \left(x_{k\tau_0}, x_{k\tau_0+\tau} \ldots, x_{k\tau_0+l\tau}, \ldots, x_{k\tau_0+(n-1)\tau}\right)$, where $k \in \mathbb{N}$, $n$ is the embedding dimension (number of values in $\mathbf{x}_k$), $\tau_0 \in \mathbb{N}_{\geq 1}$ is the delay time of the embedding vectors, $\tau \in \mathbb{N}_{\geqq 1}$ is the delay time of samples and $l + 1$ the index of $x_{k\tau_0+l\tau}$ in $\mathbf{x}_k$, $l \in \mathbb{N}$. Let $P_k$ be the permutation derived from $\mathbf{x}_k$, with $\tau_0 = 1$. $P_k = \left(\begin{smallmatrix} 1,2,3,\ldots,n \\ 5,n,1,\ldots,3 \end{smallmatrix}\right)$ for example is obtained by sorting the

values of $\mathbf{x}_k$ in ascending order, with $x_{k+4\tau} < x_{k+(n-1)\tau} < x_k < \ldots < x_{k+2\tau}$. Identical values are sorted by ascending order of their time index.

Thereafter, we convert the pseudo-source of ordinal patterns into a set of vectors of permutations or simply matrices. Indeed, given the set $\{P_k\}$ of ordinal patterns, we define another set $\{\mathbf{S}_l\}$ of matrices such that $\mathbf{S}_l = \left( P_l^T, P_{l+\tau}^T, \ldots, P_{l+(m-1)\tau}^T \right)$, where $P_l^T$ is a column vector (the transpose of $P_l$). $P_l$ is an $n$-length vector of positive integers in $\{1, 2, 3, \ldots, n\}$, while $\mathbf{S}_l$ is an $n \times m$ matrix of the same integer set, and $m$ the number of permutations considered to form $\mathbf{S}_l$. We showed in [16] that the equivalent embedding dimension for this process is $\rho = n + m - 1$.

Let us consider for example a period-5 cycle orbit obtained by generating 5 distinct random numbers $(0.8147, 0.9058, 0.1270, 0.9134, 0.6324)$ and repeating this basic sequence $K$ times $(K > 2)$. The five distinct 5-order permutations obtained by sorting the values of vectors $\mathbf{x}_k$, $k = 0$ to 4, are the following: $P_0 = \left( \frac{1,2,3,4,5}{3,5,1,2,4} \right)$; $P_1 = \left( \frac{1,2,3,4,5}{2,4,5,1,3} \right)$; $P_2 = \left( \frac{1,2,3,4,5}{1,3,4,5,2} \right)$, $P_3 = \left( \frac{1,2,3,4,5}{5,2,3,4,1} \right)$ and $P_4 = \left( \frac{1,2,3,4,5}{4,1,2,3,5} \right)$. The corresponding set of ordinal patterns for the whole time series is $\{P_l\} = \{P_0, P_1, P_2, P_3, P_4, P_0, P_1, P_2, P_3, P_4, P_0, P_1, P_2, \ldots\}$. From $\{P_l\}$, one can deduce for example the set of $5 \times 3$ matrices as $\{\mathbf{S}_l\} = \{\mathbf{S}_0, \mathbf{S}_1, \mathbf{S}_2, \mathbf{S}_3, \mathbf{S}_4, \mathbf{S}_0, \ldots\}$,

where $\mathbf{S}_0 = \begin{pmatrix} 3 & 2 & 1 \\ 5 & 4 & 3 \\ 1 & 5 & 4 \\ 2 & 1 & 5 \\ 4 & 3 & 2 \end{pmatrix}$, $\mathbf{S}_1 = \begin{pmatrix} 2 & 1 & 5 \\ 4 & 3 & 2 \\ 5 & 4 & 3 \\ 1 & 5 & 4 \\ 3 & 2 & 1 \end{pmatrix}$, $\mathbf{S}_2 = \begin{pmatrix} 1 & 5 & 4 \\ 3 & 2 & 1 \\ 4 & 3 & 2 \\ 5 & 4 & 3 \\ 2 & 1 & 5 \end{pmatrix}$, $\mathbf{S}_3 = \begin{pmatrix} 5 & 4 & 3 \\ 2 & 1 & 5 \\ 3 & 2 & 1 \\ 4 & 3 & 2 \\ 1 & 5 & 4 \end{pmatrix}$, and $\mathbf{S}_4 = \begin{pmatrix} 4 & 3 & 2 \\ 1 & 5 & 4 \\ 2 & 1 & 5 \\ 3 & 2 & 1 \\ 5 & 4 & 3 \end{pmatrix}$. Therefore, for $n = 5$ and $m = 3$, $\{\mathbf{S}_l\}$ is a set of matrices and is also 5-periodic like the generating time series $\{x_t\}$. Choosing any other value of $m \geq 1$ will output a period-5 series of matrices.

### 2.2. Recap of the conditional entropy of ordinal patterns

The PE as well as the conditional entropy of ordinal patterns (CPE) are based on the statistical analysis of probability distribution of the ordinal patterns. We showed in [16] that the CPE can be expressed as

$$ h(n) = H(s) - H(n). \tag{1} $$

$H(n)$ is the Shannon entropy of the series of permutations of order $n$ defined as

$$ H(n) = -\sum p(\Theta) \cdot \ln(p(\Theta)), \tag{2} $$

where

$$ p(\Theta) = \frac{\#\{k \mid k \leq T - n\tau, P_k = \Theta\}}{T - n\tau + 1}, \tag{3} $$

is the probability of the permutation $\Theta$ and $\#$ denotes the cardinality [5]. Similarly, $H(s)$ is the Shannon entropy related to the series of $n \times 2$ ordinal matrices $\mathbf{S}$ derived from the series of ordinal patterns. Instead of considering the probability distribution of the series of ordinal matrices as is done for the CPE, we

consider exclusively its diversity, i.e the number of distinct ordinal matrices it contains. In order words, we are not interested to the number of occurrences of (probability) an existing ordinal matrix, but only to its existence in the series.

### 2.3. Particular behavior of the number ordinal matrices

The behavior of $\Lambda$ depends on the nature of the time series under investigation. We already know that the series of matrices derived from a periodic dynamics is also periodic [16]. The upper limit of $\Lambda$ is equal to $\Lambda_{max} = (n!)^m$ if we consider each matrix as a word of $m$ symbols, and each of the possible $n!$ permutations as a distinct symbol. Therefore, the necessary data length required for an effective evaluation of the complexity of the time series also is such that $T \gg (n!)^m$.

**Theorem 1.** *Given a set $\{P_k\}$ of ordinal patterns of length $n$, the maximum number of distinct ordinal matrices $\mathbf{S}$ of size $n \times m$ that can be derived from $\{P_k\}$ is $\Lambda_0 = (n-1)!n^m$.*

*Proof.* If we consider each permutation as a distinct symbol in the ordinal matrix $\mathbf{S}$, then $\Lambda_0 = (n!)^m$. However, the structure of $\mathbf{S}$ does not allow this basic consideration. Indeed, $\mathbf{S}$ is composed of positive integers ranged from 1 to $n$ and each of its columns contains each of the $n$ integers once (columns are permutations). Thus, the number of distinct columns is $n!$. While considering the rows, each integer can appear $m$ times and the number of distinct rows is $n^m$. Therefore, the number of distinct matrices is equal to the number of distinct rows multiplied by the number of distinct columns, knowing one element in each column, hence

$$\Lambda_0 = (n-1)!n^m.$$

We can also consider that the number of distinct matrices is equal to the number of distinct columns multiplied by the number of distinct rows, knowing one element in each row, hence

$$\Lambda_0 = n!n^{m-1} = (n-1)!n^m,$$

which ends the proof. $\qquad\square$

**Theorem 2.** *Given an embedding dimension $\rho = n + m - 1$, the maximum number of distinct ordinal matrices $\Lambda_0$ satifies $\Lambda_0 < \rho!$, where $\rho!$ is the maximum number of distinct ordinal patterns of length $\rho$.*

*Proof.* We showed in Theorem 1 that $\Lambda_0 = (n-1)!n^m$. By expanding $\rho!$, we obtain

$$(n+m-1)! = (n-1)!\prod_{i=0}^{m-1}(n+i).$$

As it is evident that

$$n^m < \prod_{i=0}^{m-1}(n+i),$$

it turns out that $\Lambda_0 < \rho!$, which ends the proof. $\qquad\square$

Theorem 2 shows that the ordinal matrix transform lets us consider large embedding dimensions and to reduce the number of symbols of the corresponding alphabet. Indeed, given a one dimensional embedding dimension $\rho$ and the corresponding alphabet $\{P_k\}$ of ordinal patterns, one can decompose $\rho$ into a two dimensional embedding dimension $(n, m)$, with $\rho = n + m - 1$, such that the new alphabet $\{S_l\}$ is the set of ordinal matrices. The cardinality of $\{P_k\}$ is $\rho! = (n+m-1)!$, whereas that of $\{S_l\}$ is $\Lambda_0 = (n-1)! n^m$. The main advantage of this decomposition is the possibility of reducing the data length $T$ required for an effective complexity measure. Instead of $T \gg \rho!$, one may consider $T \gg \Lambda_0$.
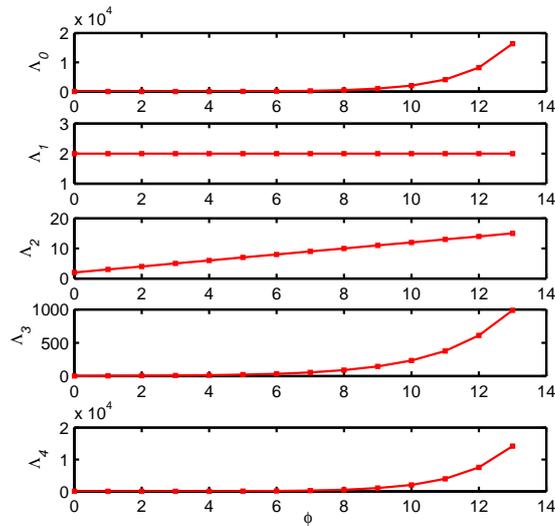


Figure 1: Particular behavior of $\Lambda$ in terms of $\phi = m - 1$. From top to bottom are shown the behavior of $\Lambda$ for a purely random source ($\Lambda_0$), periodic ($\Lambda_1$), quasi-periodic ($\Lambda_2$), chaotic ($\Lambda_3$) and stochastic data ($\Lambda_4$). We set $T = 5 \times 10^5$, $n = 2$ and $0 \leq \phi \leq 13$

Fig. 1 shows some examples of the behavior of $\Lambda$ for the particular cases of periodic, quasi-periodic, chaotic and stochastic data. The periodic and chaotic dynamics were generated using the logistic equation

$$x_{t+1} = r x_t (1 - x_t), \tag{4}$$

with $r = 3.56$ and $r = 4$ respectively, and $x_0 = 0.4$. The quasi-periodic dynamics was generated from the sine-circle map

$$\theta_{t+1} = \Omega + \theta_t + \frac{\gamma}{2\pi} \sin(2\pi\theta_t) \mod 1, \tag{5}$$

with $\gamma = 0$, $\Omega = \frac{-1+\sqrt{5}}{2}$ and $\theta_0 = 0.5$; while the stochastic sequence corresponds to white noise with a Gaussian distribution. From this figure, it is evident that $\Lambda$ is bounded by $\Lambda_0 = (2)^m$ for all four dynamics. The corresponding values are tabulated in Table 1. In the particular case of chaotic dynamics, $\Lambda$ corresponds to the sequence of the Fibonacci numbers. Furthermore, increasing the data length for given values of $n$ and $m$ does not affect the corresponding value of $\Lambda$ in the case of periodic, quasi-periodic and chaotic dynamics. This observation

Table 1: Behavior of $\Lambda$ in terms of $\phi = m - 1$ for particular dynamics, $n = 2$, $T = 5 \times 10^5$: $\Lambda_{1-4}$ for respectively the periodic, quasi-periodic, chaotic and stochastic data series.

| $\phi$ | 0 | 1 | 2 | 3 | 4 | 5 | 6 | 7 | 8 | 9 | 10 | 11 | 12 | 13 |
|---|---|---|---|---|---|---|---|---|---|---|---|---|---|---|
| $\Lambda_0$ | 2 | 4 | 8 | 16 | 32 | 64 | 128 | 256 | 512 | 1024 | 2048 | 4096 | 8192 | 16384 |
| $\Lambda_1$ | 2 | 2 | 2 | 2 | 2 | 2 | 2 | 2 | 2 | 2 | 2 | 2 | 2 | 2 |
| $\Lambda_2$ | 2 | 3 | 4 | 5 | 6 | 7 | 8 | 9 | 10 | 11 | 12 | 13 | 14 | 15 |
| $\Lambda_3$ | 2 | 3 | 5 | 8 | 13 | 21 | 34 | 55 | 89 | 144 | 233 | 377 | 610 | 987 |
| $\Lambda_4$ | 2 | 4 | 8 | 12 | 32 | 64 | 128 | 256 | 510 | 1017 | 2005 | 3923 | 7534 | 14190 |

clearly attests that each of these dynamics can be characterized by the behavior of $\Lambda$. For chaotic dynamics with $n = 2$ for example, the behavior of $\Lambda$ in terms of $m$ is bounded by the sequence of Fibonacci numbers: $\Lambda(2, m)$ is equal to the $m$-th Fibonacci number, provided $T \gg 2^m$. One can also observe that $\Lambda$ increases faster in the case of stochastic data than chaotic dynamics.

*2.4. Modeling of the behavior of $\Lambda$ as a function of $m$*

In this section, we analyze the behavior of the number of ordinal matrices in terms of the second embedding dimension $m$. While looking at Fig. 1, one can observe three types of behavior for $\Lambda$: constant, linear and exponential behavior. All these behaviors of $\Lambda$ as shown in Fig. 1 are bounded by $\Lambda_0$ and depend on the dynamics under investigation. It then follows from this observation that each type of dynamics can be characterized by the evolution rule of $\Lambda$ compared to $\Lambda_0$. For this purpose, we suggest modeling the behavior of $\Lambda$ in terms of $\phi = m - 1$ so that all the above three behaviors are taken into account. For periodic dynamics, $\Lambda(n, \phi) = a_0$ where $1 \leq a_0 \leq L$ is a positive integer related to the period of the underlying dynamics. $\Lambda$ for the quasi-periodic dynamics is bounded by $\Lambda(n, \phi) = n + \phi$. By combining the periodic and the quasi-periodic dynamics, the modeling function can be expressed as $\Lambda(n, \phi) = \mu(n + \phi)^\alpha$. For this modeling function, $\mu = a_0$ and $\alpha = 0$ for periodic dynamics; for quasi-periodic dynamics, $\mu = \alpha = 1$. The exponential behavior can also be modeled as an attenuated value of $\Lambda_0$, i.e $\Lambda(n, \phi) = \mu \cdot n^{\lambda \cdot (\phi+1)}$, where $\lambda \leq 1$. By combining the linear and exponential models, the modeling function of $\Lambda$ becomes

$$\Lambda(n, \phi) = \mu \cdot (n + \phi)^\alpha \cdot b^{\lambda \cdot (\phi+1)}, \tag{6}$$

where $\mu \in \mathbb{R}_+$ is the periodicity index, $\alpha \in \mathbb{R}$ is the quasi-periodicity index, $\lambda \in \mathbb{R}$ the index of non-regularity and $b \in \mathbb{R}_{\geq 2}$ the exponential basis.

By considering the behavior of $\Lambda = \Lambda_0$, which corresponds to a purely random source, one can easily deduce the values of $\mu$, $\alpha$ and $\lambda$ by solving the equation

$$\mu \cdot (n + \phi)^\alpha \cdot b^{\lambda \cdot (\phi+1)} = \Lambda_0. \tag{7}$$

We solved this equation and found

$$\begin{cases} \mu = (n-1)! \\ \alpha = 0 \\ \lambda = \frac{\ln(n)}{\ln(b)}. \end{cases} \tag{8}$$

Solving the same equation in the case of quasi-periodic dynamics with $\Lambda(n, \phi) = n + \phi$, we found

$$\begin{cases} \mu = 1 \\ \alpha = 1 \\ \lambda = 0. \end{cases} \tag{9}$$

For periodic dynamics, the solution is trivial

$$
\begin{cases}
\mu = a_0 \\
\alpha = 0 \\
\lambda = 0,
\end{cases}
\tag{10}
$$

with $1 \leq a_0 \leq L$. For the rest of the paper, we set $b = \exp(1)$. In that case, $\lambda_0 = \ln(n)$ is the upper limit of the nonregularity index $\lambda$.

Between the solutions presented above, there are many intermediate combinations of $\mu$, $\alpha$ and $\lambda$ which depend on the nature of the underlying dynamics. The appropriate solution $\psi = (\mu, \alpha, \lambda)$ of Eq. (6) in that case can be determined using least mean square interpolation, with $f_1(\phi) = 1$, $f_2(\phi) = \ln(n + \phi)$ and $f_3(\phi) = \phi + 1$ as the three basis functions. The values obtained are accurate as $T \to +\infty$, hence the usefulness of the asymptotic behavior. In the case for example of the particular dynamics in Fig. 1, we found respectively $\psi_1 = (2, 0, 0)$, $\psi_2 = (1, 1, 0)$, $\psi_3 = (1.2453, -0.057, 0.4876)$, and $\psi_4 = (0.9228, 0.1221, 0.6685)$ for the periodic, quasi-periodic, chaotic and stochastic sequence. $\lambda$ is close to its upper limit $\lambda_0 = \ln(n)$ as the dynamics are complex. The largest complexity value that can be estimated by this model is given in Eq. (8). Similarly to the Lyapunov exponent, we expect that regular dynamics are characterized by $\lambda \leq 0$. In this way, periodic dynamics with large periods may be easily detected as regular.

## 3. Simulation results

In this section, we apply the modeling of $\Lambda$ to well known dynamical systems and compare the results to the CPE and the Lyapunov exponent $\lambda_{Lyap}$.

### 3.1. Parameter setting

Choosing the appropriate value of the embedding dimension $n$ is crucial in the analysis of dynamical systems. In the case of ordinal pattern analysis, $n$ should be as large as possible for the CPE to approximate the KSE. In practice, the choice of $n$ should take into account the data length $T$. This requirement is also valid for the embedding dimension $m$ of the second dimension of the ordinal matrix. Furthermore, we need to consider at least four values of $m$ for the estimation error of $\mu$, $\alpha$ and $\lambda$ to be minimized. Therefore, the choice of the pair $\mathcal{C} = (n, m)$ needs to be well balanced.

In the case of nonregular dynamics, assuming that $\Lambda$ is an increasing exponential function, its first difference (with respect to $m$) $\Delta_m \Lambda(n, m) = \Lambda(n, m + 1) - \Lambda(n, m)$ also should be an increasing function. However, due to the limited value of $T$, $\Delta_m \Lambda$ increases up to a limit value, then decreases till zero. This maximum value of $\Delta_m \Lambda$ corresponds to the largest value $m_0$ of $m$ that can be considered, given $n$ and $T$. $m_0$ is the first root of

$$
\Delta_m^2 \Lambda(n, m) = 0,
\tag{11}
$$

where

$$
\Delta_m^2 \Lambda(n, m) = \Lambda(n, m + 2) + \Lambda(n, m) - 2\Lambda(n, m + 1)
\tag{12}
$$

is the second difference of $\Lambda$ with respect to $m$. Fig. 2 shows the behavior of $\Lambda$ and $\Delta_m^2 \Lambda$ in the case of the chaotic dynamics described in Fig. 1 for various
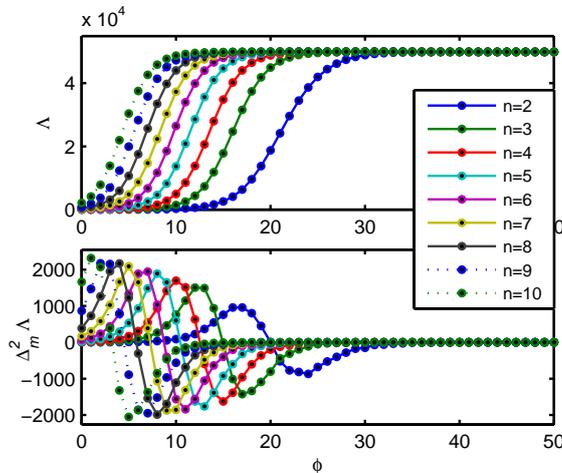
Figure 2: Appropriate choice of $n$ and $\phi = m - 1$ for $T = 5 \times 10^4$. From top to bottom are shown the behavior of $\Lambda$ and $\Delta_m^2 \Lambda$ for a chaotic time series.

Table 2: Appropriate values of $n$ and $m$ as well as the corresponding values of $\Lambda$ for $T = 5 \times 10^4$ in the case of the chaotic dynamics shown in Fig. 1.

| $n$ | 2 | 3 | 4 | 5 | 6 | 7 | 8 | 9 | 10 |
|---|---|---|---|---|---|---|---|---|---|
| $m_0$ | 22 | 16 | 14 | 12 | 10 | 9 | 7 | 6 | 5 |
| $\Lambda(n, m_0)$ | 24170 | 17800 | 20591 | 20857 | 18554 | 22343 | 17548 | 19954 | 21963 |

values of $n$ and $m$. The corresponding values of $\Lambda$ are given in Table 2. In practice, the optimal value of $m_0$ is smaller than the one corresponding to $\Delta_m^2 \Lambda = 0$. For the algorithm to be robust, we suggest to take as optimal choice the value of $m$ corresponding to the maximum of $\Delta_m^2 \Lambda(n, m)$. This value is obtained by solving

$$\Delta_m^3(n, m) = 0,$$

where

$$\Delta_m^3(n, m) = \Lambda(n, m + 3) + 3\Lambda(n, m + 1) - 3\Lambda(n, m + 2) - \Lambda(n, m)$$

is the third difference of $\Lambda$.

The optimal pair $\mathcal{C}_0 = (n_0, m_0)$ also depends on the nature of the dynamics under investigation. For periodic dynamics, large values of $n$ ($L < n < T$ for example) and $m$ can be considered for all the $L$ possible patterns to be observed [16]. For stochastic time series for example ($T = 5 \times 10^4$), using Eq. (11), we found respectively $\mathcal{C}_0 = (2, 16)$, $\mathcal{C}_0 = (3, 9)$, $\mathcal{C}_0 = (4, 6)$, $\mathcal{C}_0 = (5, 4)$ and $\mathcal{C}_0 = (6, 1)$, $\mathcal{C}_0 = (7, 1)$, $\mathcal{C}_0 = (8, 1)$, $\mathcal{C}_0 = (9, 1)$. The corresponding number of ordinal matrices are respectively 21202, 18731, 16350, 13192, 20792, 5040, 28765, 46717 and 49678. Given that only $1 \leq m \leq m_0$ is allowed for fixed $n_0$ and $T$, and that we require at least four values of $m$ for evaluating $\mu$, $\alpha$ and $\lambda$, only the first three pairs are allowed. We can also observe that $\Lambda(n_0, m_0) < \frac{T}{2}$ until the critical point $\mathcal{C}_0 = (6, 1)$ where $\Lambda(n_0, m_0) \simeq \frac{T}{10}$, and that $\Lambda(n_0, m_0) > \frac{T}{2}$ for other $n_0 > 6$. It is then obvious that there exists also an upper limit $\Lambda_{max} = \frac{T}{2}$ that should not be exceeded for an efficient estimation of $\mu$, $\alpha$ and $\lambda$. Thus, for a given $T$, we set $n$ and $m_0$ such that $\Lambda(n, m_0) \leq \frac{T}{10}$.

### 3.2. Detection of the period doubling route to chaos

The logistic map, described in Eq. (4), is useful for evaluating the efficiency of time series analysis algorithms [18]. For almost all $\mu \in (0, 4]$ the KS entropy either coincides with the Lyapunov exponent if it is positive or is equal to zero otherwise [19, 20]. It has also been shown that the Lyapunov exponent for the logistic map can be estimated rather accurately [21]. We computed the $\mu$, $\alpha$ and $\lambda$ spectrum (see Fig. 3) for the logistic map and compared the results to the CPE and the Lyapunov exponent (see Fig. 4).
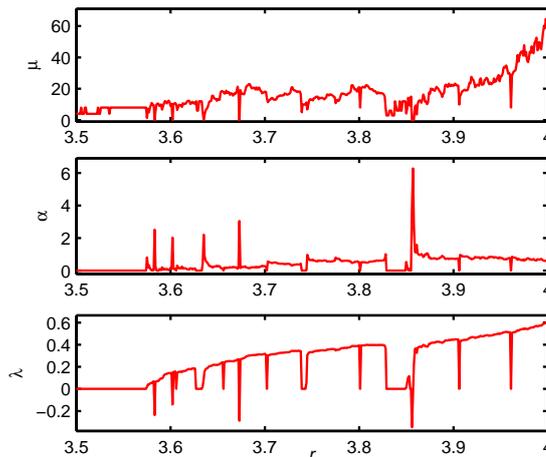


Figure 3: Spectrum of ordinal matrix indices for $n = 8$ and $T = 5 \times 10^5$. From top to bottom are shown the behavior of $\mu$, $\alpha$ and $\lambda$. $m \geq 5$ is self adapting such that $\Lambda(m) \leq \frac{T}{10}$.
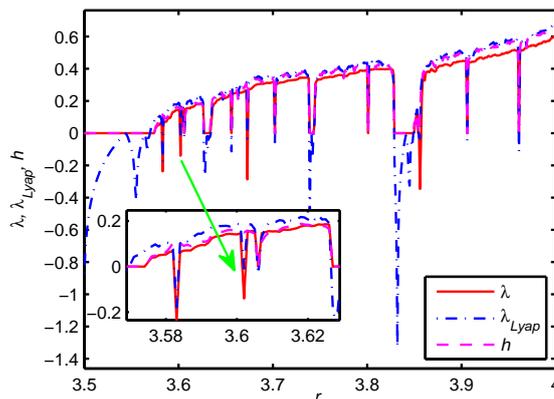


Figure 4: Comparison between $\lambda_{Lyap}$, $h$ and $\lambda$ presented in Fig. 3 for $n = 8$ and $T = 5 \times 10^5$.

Fig. 3 confirms that periodic dynamics are characterized by $\psi = (a_0 \geq 1, 0, 0)$, where $a_0 = L$ if $L \leq n$. For some particular cases where $L > n$, the dynamics is detected as $\psi = (\mu < 1, \alpha > 1, \lambda < 0)$. Some examples are given (see the zoomed region in Fig. 4) for $r = 3.583$, $r = 3.602$ and $r = 3.673$ whose

9

periods are respectively $L = 24$, $L = 88$ and $L = 20$. The corresponding detection results are $\psi = (0.0746, 2.5191, -0.2374)$, $\psi = (0.2734, 2.0271, -0.1401)$ and $\psi = (0.0213, 3.0503, -0.2875)$, respectively. It should be noted that for these values of the control parameter $r$, both $\lambda_{Lyap}$ and $\lambda$ are negative, whereas $h > 0$ instead of $h = 0$.

In Fig. 4, one can notice a quite uniform bias between the LE and the nonregularity index, whereas it is not the case for the CPE [16]. This bias can be reduced by increasing $n$ and $T$. As it is quite uniform (constant ratio between $\lambda$ and $\lambda_{Lyap}$), multiplying $\lambda$ by a scaling factor to be determined may also help reduce this bias, without affecting the detection result.

*3.3. Detection of regular dynamics with large periods*
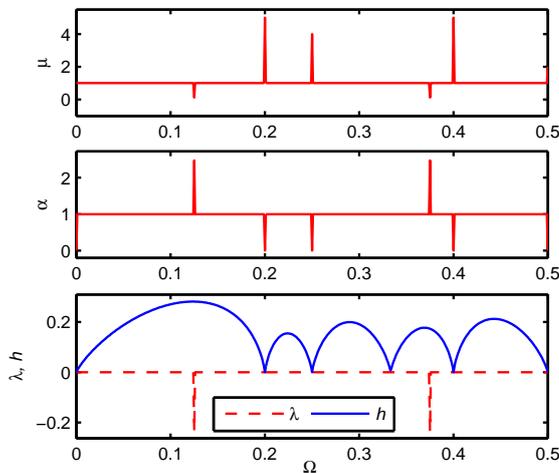


Figure 5: Detection of periodic dynamics with large periods in the rotation map. The comparison of the spectra of $\lambda$ and $h$ shows the efficiency of the proposed algorithm compared to the CPE. We set $T = 5 \times 10^4$ and $n = 5$.

We now discuss the case of dynamics with large periods. Such dynamics require large embedding dimensions $n$ for them to be detected as regular by the ordinal patterns related entropy measures. In practice, due to the limited data length, it is common to choose small embedding dimensions. It is well known that the KSE of a periodic dynamical system is equal to zero. However, the CPE in that case may output nonzero values, depending on the embedding dimension $n$ and the period $L$ of the underlying dynamics. To illustrate the efficiency of our approach, we considered the rotation map. The rotation map is obtained by setting $\gamma = 0$ in Eq. (5). When $\Omega$ is a rational number, the map provides a periodic behavior [14]. We used $T = 5 \times 10^4$ as data length, $n = 5$ as embedding dimension and $\Omega$ varying from 0 to 0.5, with step size $\Delta\Omega = 10^{-3}$. As shown on Fig. 5, all the dynamics are detected as regular by the indicators $\mu$, $\alpha$ and $\lambda$, whereas the CPE detects most of the dynamics as nonregular, thus outputting $h > 0$. We verified that $h(5)$ goes to 0 at rational numbers whose denominators are smaller than or equal to 5, which corresponds to $\Omega \in \{0, \frac{1}{5}, \frac{1}{4}, \frac{2}{5}, \frac{1}{2}\}$. Dynamics corresponding to these four values of $\Omega$ are clearly detected as periodic by our approach, thus outputting respectively $\psi_0 = (1, 0, 0)$,

$\psi_{\frac{1}{5}} = (5, 0, 0)$, $\psi_{\frac{1}{4}} = (4, 0, 0)$, $\psi_{\frac{2}{5}} = (5, 0, 0)$ and $\psi_{\frac{1}{2}} = (2, 0, 0)$. The OMCI thus correctly detects periodic dynamics with large periods without needing large embedding dimension $n$.

### 3.4. Detection of the quasi-periodic route to chaos

The interest for this type of dynamical system is to confirm the efficiency of the OMCI for the detection of regular dynamics using small values of the permutation order $n$. For this purpose, we have considered the sine circle map as defined in Eq. (5). $\Omega$ is the frequency ratio parameter and $\gamma$ the nonlinearity parameter. For $\Omega = \frac{-1+\sqrt{5}}{2}$, the system is known to exhibit quasi-periodic dynamics for $0 \leq \gamma \leq 1$ [22, 23]. As in the case of the rotation map, we
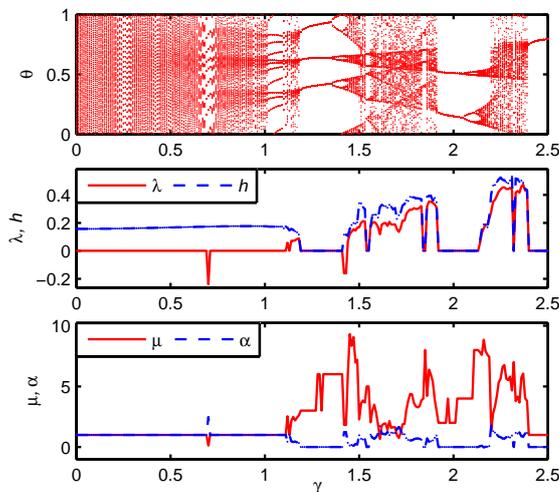


Figure 6: OMCI spectrum of the sine circle map. We set $T = 5 \times 10^4$, $n = 5$ and $0 \leq \gamma \leq 2.5$ with step size $\Delta\gamma = 0.01$. The comparison with the CPE shows a better performance for the OMCI.

considered sequences of length $T = 5 \times 10^5$ samples and the control parameter $0 \leq \gamma \leq 2.5$ varying with step size $\Delta\gamma = 0.01$. We also choose $\theta_0 = 0.4$ as initial condition and set $n = 5$. The corresponding results for the OMCI and the CPE are shown in Fig. 6 from where it is confirmed that $\lambda \leq 0$ for regular (periodic and quasi-periodic) dynamics. We can thus conclude that chaos indicators based on the behavior of $\Lambda$ efficiently detect regular dynamics, using small embedding dimensions, which also makes it possible to use small data lengths.

### 3.5. Distinguishing between deterministic and stochastic data

The combination of the three indices can also help to distinguish between deterministic and stochastic data, provided that the different parameters are suitably chosen. Figure 7 shows some examples of detection results obtained for stochastic time series. Stochastic data are random sequences with a Gaussian distribution, whose standard deviation is $\sigma = 1$ and mean value $\bar{\eta} = 0$. From this figure, it turns out that stochastic data are characterized by $\psi = (\mu \to (n-1)!, \alpha \to 0, \lambda \to \ln(n))$, as theoretically predicted.

In order to verify this property, we considered different values of $n$. Given the the large complexity of stochastic data, increasing $n$ imposes large values

11
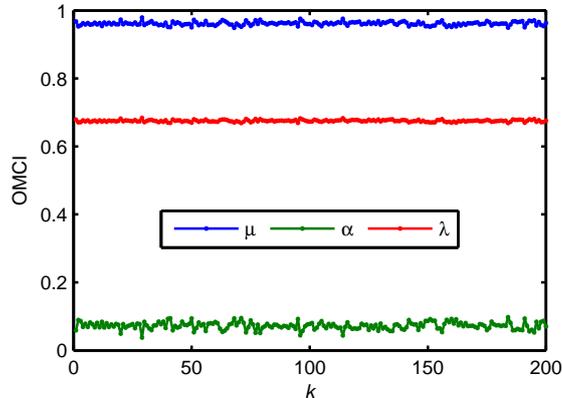
Figure 7: OMCI spectrum for stochastic data with Gaussian distribution. We generated 200 sequences of length $T = 5 \times 10^4$ and set $n = 2$. For this source to be considered as purely random, it is necessary that $\mu \to 1$ and $\alpha \to 0$, which is not actually the case.

of $T$. We thus set $n \in \{2, 3, 4\}$ and $T = 10^7$. For comparison purpose, we also considered a chaotic dynamics from the logistic map with $r = 4$. The corresponding results are respectively $\psi_2 = (1.2136, -0.0224, 0.4827)$, $\psi_3 = (2.7878, 0.0345, 0.5596)$ and $\psi_4 = (5.1711, 0.2086, 0.5759)$ for the chaotic dynamics; and $\psi_2 = (0.9085, 0.1283, 0.6708)$, $\psi_3 = (1.7790, 0.1192, 1.0763)$ and $\psi_4 = (6.0059, -0.0007, 1.3863)$ for the stochastic data. By comparing the values of $\lambda$ for the two types of dynamics, in appears that $\lambda < \ln(2)$ for the chaotic dynamics, while $\lambda$ for the stochastic data significantly increases with $n$ as $\lambda \simeq \ln(n)$. This high sensitivity of $\lambda$ to $n$ in the case of stochastic data may be helpful for distinguishing between deterministic and stochastic data. It should also be noted that for suitably chosen values of $m$, $\mu \to (n-1)!$ for stochastic data and $\mu > (n-1)!$ for chaotic data. An interesting remark is related to the useful data length. Indeed, considering that for stochastic processes $\lambda = \ln(n)$, the required data length may be set as $T \gg n^m$, which is much smaller than $T \gg (n!)^m$ and $T \gg \rho!$, $\rho = n+m-1$ being the equivalent embedding dimension [16]. Thus, choosing $T \gg \rho!$ is sufficient in some cases.

We also applied the algorithm to the random walk with $T = 10^5$ and $n \in \{2, 3, 4, 5, 6, 7, 8\}$. The results obtained are tabulated in Table 3. From this table, it turns out that the random walk is characterized by $\lambda = \ln(2)$, $\alpha = 0$ and $\mu = 2^{n-2}$. The evolution rule of its number of ordinal matrices can then be expressed as

$$\lim_{T \to \infty} \Lambda(n, m) = 2^{n+m-2}. \tag{13}$$

Table 3: Characterization of the random walk by the OMCI. The data length is set to $T = 10^5$ while $n \in \{2, 3, 4, 5, 6, 7, 8\}$.

| $n$ | 2 | 3 | 4 | 5 | 6 | 7 | 8 |
|---|---|---|---|---|---|---|---|
| $m_0$ | 9 | 8 | 7 | 6 | 5 | 5 | 5 |
| $\mu$ | 1 | 2 | 4 | 8 | 16 | 32 | 64 |
| $\alpha$ | 0 | 0 | 0 | 0 | 0 | 0 | 0 |
| $\lambda$ | $\ln(2)$ | $\ln(2)$ | $\ln(2)$ | $\ln(2)$ | $\ln(2)$ | $\ln(2)$ | $\ln(2)$ |

12

By setting for example $T = 6^9$, $n \in \{2, 3, 4, 5, 6\}$ and $m = 3$, we also verified that pseudorandom data with Gaussian and uniform distributions generated from MATLAB are characterized by $\lambda = \ln(n)$, $\alpha = 0$ and $\mu = (n - 1)!$ as predicted. However, while setting $m > 4$ and $n > 4$, we obtained $\mu < \ln(n-1)!$, $\alpha > 0$ and $\lambda < \ln(n)$, thus attesting that the complexity of the random data series is less than that of a purely random source. We can thus confirm that a data source is purely random only if

$$\lim_{T \to \infty} \Lambda(n, m) = (n - 1)! n^m. \tag{14}$$

Applying this relation to Eq. (4), it turns out that the upper limit of the CPE for a purely random source is $\ln(n)$.

Now applying the algorithm to the "handel.mat" audio file downloaded from MATLAB ($T = 73113$), we found the same result as for the Gaussian and uniform distribution noises for $n \in \{2, 3, 4\}$ and $m = 3$. While setting $n = 5$, we found $\psi_5 = (0.0036, 6.1822, 0.4756)$ indicating a false detection, which clearly attests that we need to increase the data length. However, while using the same data length for the MATLAB pseudorandom sequences, the variation law of $\Lambda$ in Eq. (14) still remains valid. It then turns out that the audio data sequence is much more random than the MATLAB pseudorandom sequences. This observation shows that OMCI can also be used for classifying stochastic data.

While considering the same parameter setting for the chaotic sequence generated from the logistic map with $r = 4$, we found $(n - 1)! < \mu < n!$, $\alpha \neq 0$ and no particular relation for $\lambda$, except that $\lambda$ is bounded by an upper limit equal to $\ln(2)$. Indeed, given that the complexity of the chaotic sequence is less than $\ln(2)$, the decrease of $\lambda$ is compensated by an increase of $\mu$, thus giving $\mu > (n - 1)!$. Considering these results, we propose the following classification in Table 4 for distinguishing between deterministic and stochastic data.

Table 4: Classification of deterministic and stochastic data. OMCI values correspond to the asymptotic behavior of the number of ordinal matrices.

| Data type | Stochastic | Deterministic | |
|---|---|---|---|
| | | Regular | Chaotic |
| Characteristics | $\mu \to (n-1)!$ $\alpha \to 0$ $\lambda \to \ln(n)$ | $\lambda \leq 0$ | $\mu > 0$ $\alpha > 0$ $0 < \lambda < \ln(n)$ |

Given that we used the least mean square approximation for determining the OMCI, the approximation error should also be taken into account. Such errors can have a significant impact for example in the case of weak chaos and some quasi-periodic dynamics where the Lyapunov exponent is close to zero.

## 4. Conclusion

In this paper, we presented a new algorithm based on the modeling of the behavior of the number of distinct ordinal matrices. This approach lets us perform both the detection of regular dynamics and the complexity measure in time series, as for the LE. In the case of one dimensional systems, the nonregularity index $\lambda$ defined here behaves similarly to the LE, thus taking negative or

zero values for regular dynamics. We did not take into account the probability distribution, which contributes to reducing the embedding dimension required for detecting regular dynamics, hence to reduce the required data length compared to the CPE. Simulation results show that the CPE converges faster to the KSE for nonregular dynamics, while the nonregularity index lets us easily detect regular dynamics. We also showed that the modeling approach can help to distinguish between chaotic and stochastic data. We proposed some modeling behaviors of $\Lambda$ for the random walk and purely random sources. The choice of $n$ depends on the nature of the data series under investigation. We verified the nonregularity index tracks the LE with a uniform bias that can be reduced by increasing the permutation order $n$ or by defining a constant scaling factor. This particular relationship between the LE and the nonregularity will be investigated in a future work.

## Acknowledgements

## References

[1] W. Barnett, A. Serletis, Martingales, nonlinearity and chaos, journal of economic, Dynamics and Control 24 (2000) 703–724.

[2] S. Chaudhury, A. Smith, B. Anderson, S. Ghose, P. Jessen, Deterministic nonperiodic flow, J. Atmos. Sci. 20 (1963) 130141.

[3] S. Chaudhury, A. Smith, B. Anderson, S. Ghose, P. Jessen, Quantum signatures of chaos in a kicked top, Nature 461 (2009) 768771.

[4] L. Glas, Introduction to controversial topics in nonlinear science: Is the normal heart rate chaotic?, Chaos 19 (2009) 0285014.

[5] C. Bandt, B. Pompe, Permutation entropy: A natural complexity measure for time series, Physical review letters 88 (2002) 174102.

[6] J. M. Amigó, Permutation complexity in dynamical systems, Springer, 2010.

[7] C. Bian, C. Qin, Q. D. Y. Ma, Q. Shen, Modified permutation-entropy analysis of heartbeat dynamics, Phys. Rev. E 85 (2012) 021906.

[8] B. Fadlallah, J. Príncipe, B. Chen, A. Keil, Weighted-permutation entropy: An improved complexity measure for time series, Phys. Rev. E 87 (2013) 022911.

[9] Z. Li, G. Ouyang, D. Li, X. Li, Characterization of the causality between spike trains with permutation conditional mutual information, Phys. Rev. E 84 (2011) 021929.

[10] X. Li, S. Cui, L. Voss, Using permutation entropy to measure the electroencephalographic effects of sevoflurane, Anesthesiology 109 (2008) 448–456.

[11] X. Li, G. Ouyang, D. Richards, Predictability analysis of absence seizures with permutation entropy, Epilepsy Res. 77 (2007) 70–74.

[12] A. Bruzzo, B. Gesierich, M. Santi, C. Tassinari, N. Bir-baumer, G. Rubboli, Permutation entropy to detect vigilance changes and preictal states from scalp EEG in epileptic patients: a preliminary study, Neurol. Sci. 29 (2008) 3–9.

[13] Y. Cao, W. Tung, J. Gao, V. Protopopescu, L. Hively, Detecting dynamical changes in time series using the permutation entropy, Phys. Rev. E 70 (2004) 046217.

[14] V. A. Unakafov, K. Keller, Conditional entropy of ordinal patterns, Physica D 269 (2014) 94–102.

[15] J. S. A. E. Fouda, W. Koepf, Detecting regular dynamics from time series using permutations slopes, Commun. Nonlinear Sci. Numer. Simulat. 27 (2015) 216–227.

[16] J. S. A. E. Fouda, W. Koepf, S. Jacquir, The ordinal Kolmogorov-Sinai entropy: A generalized approximation, Commun. Nonlinear Sci. Numer. Simulat. 46 (2017) 103–115.

[17] J. S. A. E. Fouda, Applicability of the permutation largest slope entropy to strange nonchaotic attractors, Nonlinear Dyn. (2016) 10.1007/s11071–016–3158–6.

[18] P. Collet, J.-P. Eckmann, Iterated Maps on the Interval as Dynamical Systems, Birkhäeuser, Boston, 1980.

[19] L.-S. Young, Entropy in Dynamical Systems, Princeton University Press, Princeton, 2003.

[20] M. Martens, T. Nowicki, Invariant measures for lebesgue typical quadratic maps, Astérisque 261 (2000) 239–252.

[21] J. Sprott, Chaos and Time-Series Analysis, Oxford University Press, Oxford, 2003.

[22] J. S. A. E. Fouda, W. Koepf, Efficient detection of the quasi-periodic route to chaos by the trhee-state test, Nonlinear Dyn. 78 (2014) 14771487.

[23] O. Afsar, G. Bagei, U. Tirnakli, Renormalized entropy for one dimensional discrete map: Periodic and quasiperiodic route to chaos and their robustness, Eur. Phys. J. 86 (2013) 307320.